

# Adverse effects of methylene blue in peripheral neurons: An *in vitro* electrophysiology and cell culture study

Molecular Pain  
Volume 18: 1–12  
© The Author(s) 2022  
Article reuse guidelines:  
[sagepub.com/journals-permissions](https://sagepub.com/journals-permissions)  
DOI: 10.1177/17448069221142523  
[journals.sagepub.com/home/mpx](https://journals.sagepub.com/home/mpx)  


Megan L Uhelski<sup>1,#</sup>, Malcolm E Johns<sup>2,#</sup>, Alec Horrmann<sup>2</sup>, Sadiq Mohamed<sup>2</sup>,  
Ayesha Sohail<sup>2</sup> , Iryna A Khasabova<sup>3</sup>, Donald A Simone<sup>3</sup>, and Ratan K Banik<sup>2</sup> 

## Abstract

Methylene blue (MB) is an effective treatment for methemoglobinemia, ifosfamide-induced encephalopathy, cyanide poisoning, and refractory vasoplegia. However, clinical case reports and preclinical studies indicate potentially neurotoxic activity of MB at certain concentrations. The exact mechanisms of MB neurotoxicity are not known, and while the effects of MB on neuronal tissue from different brain regions and myenteric ganglia have been examined, its effects on primary afferent neurons from dorsal root ganglia (DRG) have not been studied. Mouse DRG were exposed to MB (0.3–10  $\mu$ M) *in vitro* to assess neurite outgrowth. Increasing concentrations of MB (0.3–10  $\mu$ M) were associated with neurotoxicity as shown by a substantial loss of cells with neurite formation, particularly at 10  $\mu$ M. In parallel experiments, cultured rat DRG neurons were treated with MB (100  $\mu$ M) to examine how MB affects electrical membrane properties of small-diameter sensory neurons. MB decreased peak inward and outward current densities, decreased action potential amplitude, overshoot, afterhyperpolarization, increased action potential rise time, and decreased action potential firing in response to current stimulation. MB induced dose-dependent toxicity in peripheral neurons, *in vitro*. These findings are consistent with studies in brain and myenteric ganglion neurons showing increased neuronal loss and altered membrane electrical properties after MB application. Further research is needed to parse out the toxicity profile for MB to minimize damage to neuronal structures and reduce side effects in clinical settings.

## Keywords

methylene blue, neurotoxicity, neurite, dorsal root ganglion, dorsal root ganglion, immunocytochemistry

## Introduction

The aniline-based dye methylene blue (MB) was originally intended for use in the textile industry, but was later found to be useful in the laboratory as a marker for cell viability and Gram staining of microorganisms and in clinical settings as an antiseptic.<sup>1</sup> MB has been widely used for a variety of clinical conditions, including methemoglobinemia, ifosfamide-induced encephalopathy,<sup>2</sup> refractory vasoplegia,<sup>3</sup> cyanide poisoning,<sup>4</sup> and for a variety of surgical procedures such as staining to map sentinel lymph nodes for biopsy in breast cancer,<sup>5</sup> epithelial staining prior to biopsy collection during endoscopy for identification of tissue metaplasia or dysplasia in Barrett's esophagus,<sup>6</sup> visualizing abnormalities in bladder mucosa of patients with a history of bladder cancer,<sup>7</sup> and visually confirming urine flow after percutaneous kidney

stone removal.<sup>8</sup> In addition, there are 52 clinical trials registered in the United States ([clinicaltrials.gov](https://clinicaltrials.gov); National

<sup>1</sup>Department of Pain Medicine, The University of Texas M.D. Anderson Cancer Center, Houston, TX, USA

<sup>2</sup>Department of Anesthesiology, School of Medicine, University of Minnesota, Minneapolis, MN, USA

<sup>3</sup>Department of Diagnostic and Biological Sciences, School of Dentistry, University of Minnesota, Minneapolis, MN, USA

<sup>#</sup>contributed equally to this project.

### Corresponding Author:

Ratan K Banik, Department of Anesthesiology, University of Minnesota, B515 Mayo Memorial Building, 420 Delaware Street S.E., MMC 294, Minneapolis, MN 55455, USA.  
Email: [talktoratan@gmail.com](mailto:talktoratan@gmail.com)



Creative Commons Non Commercial CC BY-NC: This article is distributed under the terms of the Creative Commons Attribution-NonCommercial 4.0 License (<https://creativecommons.org/licenses/by-nc/4.0/>) which permits non-commercial use, reproduction and distribution of the work without further permission provided the original work is attributed as specified on the SAGE

and Open Access pages (<https://us.sagepub.com/en-us/nam/open-access-at-sage>).

Institute of Health) to investigate the clinical utility of MB for a variety of disorders, including depression,<sup>9,10</sup> bipolar disorder,<sup>11</sup> Alzheimer's disease,<sup>12</sup> and Parkinson's disease.<sup>13</sup> Indeed, MB has been included in the World Health Organization<sup>14</sup>'s list of essential medications. MB has been shown to inhibit arterial smooth muscle relaxation in response to vasodilators.<sup>15,16</sup> Although some studies suggest that this is mediated through inhibition of guanylate cyclase, its inhibition of nitric oxide synthesis is more potent and direct.<sup>15,17-20</sup> MB is also a cholinesterase inhibitor with some affinity for muscarinic binding sites,<sup>21</sup> and its metabolite, Azure B, is a potent monoamine oxidase inhibitor.<sup>22</sup>

Although MB has been generally considered to be a safe drug, there have been several reports of cytotoxicity and neurotoxicity. These include hemolytic anemia,<sup>23</sup> phototoxicity,<sup>24</sup> and central nervous system apoptosis.<sup>25</sup> One case report described the rapid onset of pain and paresthesia, followed by eventual paralysis and loss of vision and smell after lumbar subarachnoid administration of MB, findings which were associated with markers of inflammation in the spinal fluid.<sup>26</sup> A neuromuscular assessment in a patient who experienced radiculomyelopathy after lumbar MB indicated the presence of denervation.<sup>27</sup> Paralysis and leptomeningeal inflammation following epidural MB in cats were associated with inflammation of myelin sheaths and nerve roots, also suggesting potential for peripheral nervous system damage.<sup>28</sup> The precise cellular and molecular mechanisms responsible for MB-induced peripheral neurotoxicity remains unknown. Given the widespread use of this drug, it is important to elucidate mechanisms and conditions underlying neurotoxicity. Therefore, we determined the acute effect of MB on the structure and membrane electrical properties of cultured rodent dorsal root ganglia (DRG) neurons using a wide range of MB concentrations. Cultured rodent DRG neurons have been used previously to assess the toxicity of chemotherapy drugs by quantifying differences in neuronal morphology, including neurite outgrowth, following drug exposure.<sup>29,30</sup> By quantifying the proportion of cells that develop neurite outgrowth following exposure to varying concentrations of MB, a dose-response curve can be generated to determine the physiological effects of MB on neuronal health. As neurite outgrowth requires complex coordination between the growth cone and environmental signals, neurite outgrowth was used as an indicator of toxicity following exposure to MB.<sup>31, 32</sup> In addition, we performed patch clamp electrophysiology on cultured rat DRG neurons to determine if exposure to MB altered membrane electrical properties.

## Materials and methods

### Subjects

All experimental protocols were approved by the Institutional Animal Care and Use Committees at the University of

Minnesota and at the University of Texas MD Anderson Cancer Center. All studies adhered to the NIH Guide for the Care and Use of Laboratory Animals.

For immunocytochemistry experiments, adult male C3H mice ( $n = 3$ ) were obtained from Charles River (Kingston, NY) and housed in temperature- and light-controlled (12-h light/dark cycle) conditions with food and water available ad libitum.

For patch clamp electrophysiology studies, adult Sprague-Dawley rats of both sexes ( $n = 4$ ) were obtained from Harlan (Houston, TX) and housed in temperature- and light-controlled (12-h light/dark cycle) conditions with food and water available ad libitum.

### Drugs

A 1 mM stock solution of MB (Sigma Aldrich) was prepared in 50 mL PBS at pH 7.4. After mixing for 1 h, the solution was filtered through a 0.22  $\mu\text{m}$  filter. For experiments using mouse DRG neurons, a 100X solution was made from the 1 mM stock using phosphate-buffered saline (PBS), then further diluted using PBS, before the final dilution in culture media to 0.3  $\mu\text{M}$ , 1  $\mu\text{M}$ , 3  $\mu\text{M}$ , and 10  $\mu\text{M}$ . PBS only was added to the 0  $\mu\text{M}$  control wells. For rat DRG neuron electrophysiology studies, the 1 mM stock was diluted using PBS and before the final dilution in extracellular bath solution to 100  $\mu\text{M}$ .

### Cell culture

Cultures of DRGs were prepared as described previously with slight modifications.<sup>33</sup> Laminin (Sigma) and Voller's Carbonate Buffer (1:20) were added to each well of an 8-well slide (Fisher) and incubated at 4°C overnight. The next day, mice ( $n = 3$ ) were anesthetized with isoflurane then decapitated and sanitized using 70% ethanol. DRGs (10–12) were removed and placed into Puck's solution (without  $\text{Ca}^{2+}$ ,  $\text{Mg}^{2+}$ ) on ice and nerve roots were removed if necessary. In a flow hood, tissue was transferred to media containing 1:1 Ham's F-12/DMEM supplemented with 100 mM L-glutamine (Sigma) and 0.41 U/mL Collagenase-D (Roche) and placed in a humidified incubator with 5%  $\text{CO}_2$  at 37°C for 1 h. The media was decanted, replaced, and incubation continued for another hour. The laminin-coated wells were transferred to the same incubator at this time. The media and DRG tissue were then transferred to a sterile 15 mL tube using a large glass Pasteur pipette. The tissue was gently triturated 5 times, then spun down at 1000 r/min for 5 min at 4°C. The media was removed and replaced by the final media, which contained 1:1 Ham's F-12/DMEM supplemented with 40 mM glucose (Sigma), 4 mM L-glutamine, 5% Horse Serum (Gibco), 100U/mL penicillin/100  $\mu\text{g}/\text{mL}$  streptomycin (Gibco), and a large Pasteur pipette was used to triturate 10 times before a second centrifugation. In a sterile tube, 1.5 mg/mL of DNase 1 (Sigma) was added to final media. The final media was then replaced with the final media + DNase 1 solution and the DRG

tissue triturated 30 times each with the large Pasteur pipette followed by a small Pasteur pipette. Laminin was decanted from the 8-well slides, and between 150 and 300  $\mu\text{L}$  of final media was added to each of the laminin-coated wells along with the dissociated DRG tissue until a confluence of 40–60% was achieved. MB in PBS (pH 7.4) was added for a final concentration of 0  $\mu\text{M}$ , 0.3  $\mu\text{M}$ , 1  $\mu\text{M}$ , 3  $\mu\text{M}$ , or 10  $\mu\text{M}$ . Cells were then incubated at 37°C in 5%  $\text{CO}_2$  for 16 h. The dose-response experiment was repeated twice with pooled suspension of 10–12 DRGs from 1 or 2 mice.

### DRG immunocytochemistry

Following overnight incubation, culture media was removed and cells were fixed in 4% paraformaldehyde for 30 min. The slides were then washed with PBS 3 times for 10 min each time, and 300  $\mu\text{L}$  of block solution (PBS, 0.3% Triton X-100, 5% Normal Donkey Serum) was added and the cells incubated for one hour. The block solution was decanted, and plastic wells removed. Cells were then incubated overnight in a humidifying chamber with 50  $\mu\text{L}$  of primary antibody solution (PBS, 0.003% Triton X-100, 5% normal donkey serum) with anti-PGP 9.5 (AbCam 1:200). The next day, the primary antibody solution was removed, and the wells washed 3 times with PBS for 10 min. Cells were then incubated for 1 h with a secondary antibody solution (1:500 donkey anti-rabbit Cy3, Jackson Laboratories). After the solution was removed, the slides were washed 3 times with PBS for 10 min. The gel around each well was removed and the cells dehydrated by placing them in increasing concentrations of ethanol, starting at 50%, then 70%, 80%, 90%, 95%, and 100%, for 5 min each. The slide was then cleared using xylene before DPX Mountant (Sigma) and a glass coverslip were applied. Dried slides were imaged using a Leica Thunder microscope. The whole area of each well was imaged so that all DRG cells were captured. Cells were counted manually. Following a method similar to that of previous literature, DRG neurons were distinguished from debris based on their size and shape, similar to those described previously.<sup>33</sup> Neurons were classified based on the presence or absence of neurites. As multiple cells would occasionally clump together, these groups were always counted as only two cells. Any cells overhanging the edge of a picture were not counted, as neurite outgrowth could have been missed.

Each slide was digitized and split up into a series of images that could then be manually counted while the experimenter was blinded to condition. Initially, multiple blinded researchers counted the DRG neurons in each set of images and the counts were averaged between observers. No significant variations in DRG neuron counts were observed among the researchers, and thus a single individual counted the remaining well slides.

### DRG electrophysiology

Glass coverslips (12 mm diameter) were added to the chambers of a six-well plate, coated with poly-L-lysine and placed in an incubator overnight. The plate was washed with distilled water, and the coverslips positioned in the center of each well and the plate placed in an incubator. Adult male ( $n = 2$ ) and female ( $n = 2$ ) Sprague-Dawley rats were deeply anesthetized with SomnaSol (pentobarbital 390 mg/mL and phenytoin 50 mg/mL) and perfused with chilled saline on ice. Both pairs of the L4 and L5 DRG were excised and placed in a culture dish containing trypsin (0.0625 mg/mL, Hyclone) and type IA collagenase (1 mg/mL, Sigma-Aldrich) in Dulbecco's Modified Eagle Medium (DMEM). The dish was shaken in a heated chamber for 50 min at 37°C. The cells were then washed and mechanically dispersed. The suspension was filtered through a 70  $\mu\text{m}$  cell strainer and centrifuged at 180 RCF for 5–7 min at 23°C. The supernatant was removed and the cell pellet resuspended in 600  $\mu\text{L}$  of warm culture media (DMEM with 10% fetal bovine serum). The 6-well plate containing poly-L-lysine-coated wells was removed from the incubator. Glass cylinders (8 mm height, 6 mm inner diameter, 8 mm outer diameter) were placed in the center of each glass coverslip, and 100  $\mu\text{L}$  of cell suspension was added to each. Warmed culture media (500  $\mu\text{L}$ ) was then placed into each well outside the glass cylinder. After 40 min, the cylinders were carefully removed, and the plate was incubated overnight.

Whole cell patch recording was performed on rat DRG neurons as described previously.<sup>34</sup> Glass coverslips were lifted and transferred to a recording chamber and perfused at 2 mL/min with oxygenated (95%  $\text{O}_2$  + 5%  $\text{CO}_2$ ) extracellular solution containing 117 mM NaCl, 3.6 mM KCl, 1.2 mM  $\text{NaH}_2\text{PO}_4 \cdot \text{H}_2\text{O}$ , 2.5 mM  $\text{CaCl}_2$ , 1.2 mM  $\text{MgCl}_2$ , 25 mM  $\text{NaHCO}_3$  and 11 mM glucose adjusted to pH 7.4 with NaOH. Glass micropipettes (6–8 M $\Omega$ ) were filled with an internal solution of 135 mM K-gluconate, 5 mM KCl, 5 mM Mg-ATP, 0.5 mM  $\text{Na}_2\text{GTP}$ , 5 mM HEPES, 2 mM  $\text{MgCl}_2$ , 5 mM EGTA, and 0.5 mM  $\text{CaCl}_2$  adjusted to pH 7.4 with KOH and an osmolarity of 290–300 mOsm. Only small-diameter ( $\leq 30 \mu\text{m}$ ) neurons with a resting membrane potential of at least  $-40$  mV, stable baseline recordings, and evoked spikes that overshoot 0 mV were used for further experiments and analysis. Series resistance ( $R_s$ ) was compensated to above 70%. All recordings were made at room temperature. Whole cell recordings were completed within 20–28 h after plating. DRG neurons were held at 0 pA to record spontaneous activity for 5 min. Neurons were then held at  $-60$  mV, and activation was evoked with a 15 ms step to potentials ranging from  $-50$  to  $+90$  mV in 10 mV increments. Current density was calculated by normalizing maximal peak currents with cell capacitance. This was followed by a series of 300 ms depolarizing current injections in 10 pA steps, starting from

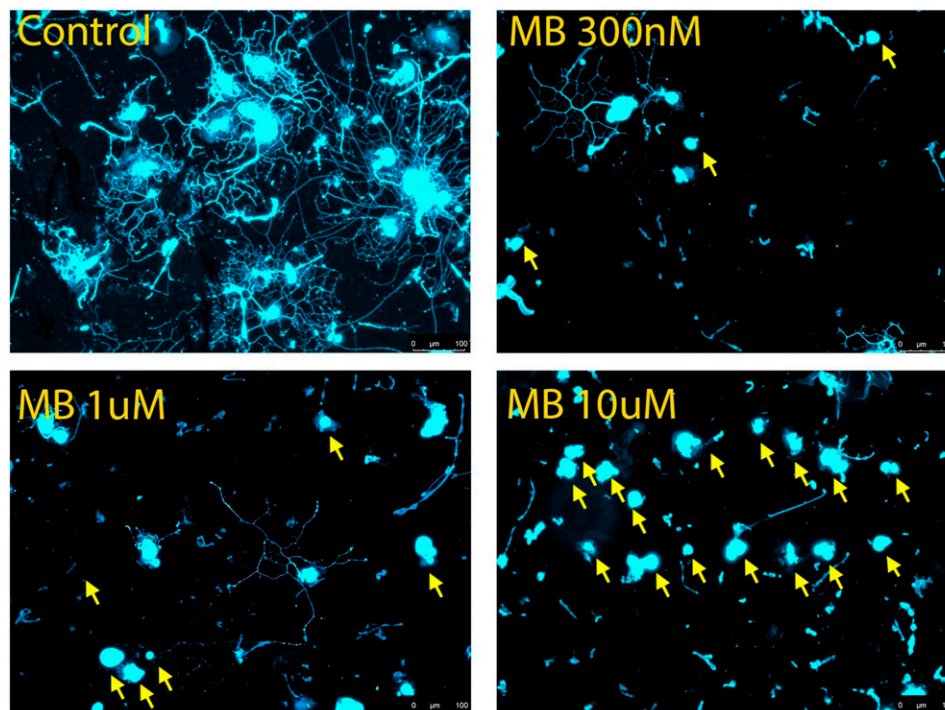


**Figure 1.** Cytotoxicity of methylene blue in cultured mouse dorsal root ganglion (DRG) neurons. Approximately  $1.1 \times 10^3$  DRG cells were seeded in each well of an 8 well slide along with methylene blue at different concentrations for 16 h. Immunocytochemistry was performed using anti-PGP 9.5 and neurite outgrowth in each well viewed under fluorescence microscope. Representative images for each concentration except 3  $\mu$ M are shown: (A) control, 0  $\mu$ M; (B) MB 0.3  $\mu$ M; (C) MB 1  $\mu$ M; (D) MB 10  $\mu$ M. Neurons without neurite extensions are indicated by yellow arrows. Scale bar represents 100  $\mu$ m.

–50 pA until an action potential was evoked. The current that induced the first action potential was defined as the current threshold (1X rheobase). Neurons were then stimulated with 2 s current injections at 1X, 2X, and 3X rheobase. MB (100  $\mu$ M) was then perfused into the bath solution at 2 mL/min for 10 min. After a 10 min washout period, post-drug maximal peak currents, current threshold, and responses to current stimulation were assessed.

### Statistical analysis

All data are expressed as percentages or mean  $\pm$  standard error of the mean. For DRG immunocytochemistry experiments, the proportion of neurons with neurites present or absent was calculated for each MB concentration (0–10  $\mu$ M) and expressed as a percentage of the total number of cells. The half maximal effective concentration (EC50), or concentration that produced 50% of neurons with an absence of neurites, was calculated using probit analysis (see <https://probitanalysis.wordpress.com/> for formulae), from which regression analysis was used to derive EC50 values.<sup>35</sup>

For DRG neuron patch clamp electrophysiology studies, peak inward current density (pA/pF) and peak outward current density (pA/pF) were compared before and after application of MB using repeated measures analysis of

variance (ANOVA), with treatment and stimulus level as within-subjects factors. Bonferroni *t*-tests were used to identify significant differences between groups. Current thresholds (rheobase, in pA), resting membrane potential (RMP, in mV), and action potential (AP) characteristics at rheobase were compared before and after treatment with MB using dependent *t*-tests. Responses to current stimulation at 1X, 2X and 3X rheobase were compared using repeated measures ANOVA (followed by Bonferroni *t*-tests) with treatment and stimulus level (1X, 2X, and 3X) as within-subjects factors. For all analyses,  $p < 0.05$  was considered significant.

## Results

### MB produced concentration-dependent decrease in neurite outgrowth in DRG neurons

Differences in proportion of neurons with neurite outgrowth was used as the parameter to evaluate neurotoxicity.<sup>36</sup> MB was administered at concentrations ranging from 0.3 to 10  $\mu$ M. The half maximal effective concentration (EC50) for neurite growth inhibition was determined from the concentration response curve for the proportion of cells without neurite extensions. In dissociated mouse DRGs, the concentration of MB that produced the highest level of

**Table 1.** Cell counts for cultured mouse DRG neurons after Methylene Blue treatment.

Methylene blue concentration, $\mu\text{M}$	Average % with neurites present	Average % with neurites absent
0	44.625	55.375
0.3	42.995	56.675
1	25.41	74.59
3	13.21	86.845
10	2.245	97.755

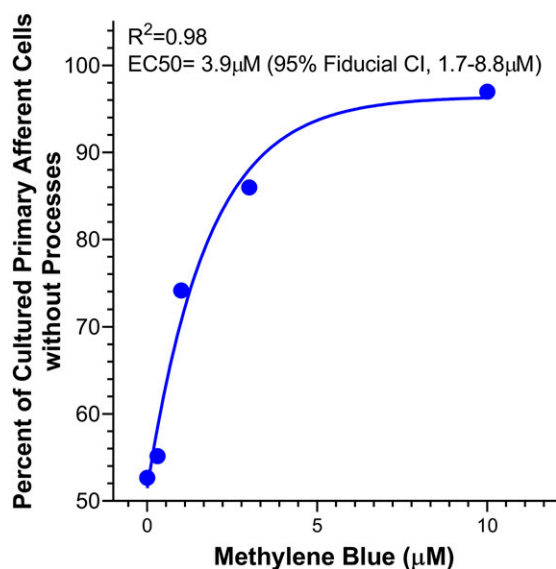
cytotoxicity was 10  $\mu\text{M}$ , the highest concentration used. At this concentration, nearly all observed cells were found to be devoid of neurite outgrowth (Figure 1). The percentage of DRG neurons with neurites ranged from a high of approximately 50% in the 0  $\mu\text{M}$  control wells to a low of about 2% with the 10  $\mu\text{M}$  MB concentration (Table 1).

The control wells showed similar neurite outgrowth to those seen in previous studies using ex vivo mouse DRGs.<sup>33</sup> Although neurite length was not measured quantitatively, a trend was observed that increasing concentrations of MB resulted in generally shorter and less dense neurite outgrowth.

The EC<sub>50</sub> of MB was found to be 3.9  $\mu\text{M}$  based on a regression analysis comparing the number of cells devoid of neurite outgrowth to the number of cells without neurite outgrowth in the control wells (Figure 2). This was done by normalizing the number of neurons with neurites absent to that of the control as a baseline survival rate. While in the first trial the number of cells added to each well was  $5 \times 10^2$ , and in the second trial approximately  $1 \times 10^3$  cells were added to each well, there was no statistically difference in the ratio of neurons with neurites present or absent between the two trials.

### MB decreased peak inward and outward current density and altered AP characteristics in cultured rat DRG neurons

Given the acute nature of the electrophysiology experiments, we used a higher concentration of MB (100  $\mu\text{M}$  for 10 min) compared to that used in culture (0.3  $\mu\text{M}$ –10  $\mu\text{M}$  for 16 h) based on previous reports indicating that acute effects of MB on rat hippocampal neurons were detectable at 10  $\mu\text{M}$  with a stronger impact on sodium currents at 100  $\mu\text{M}$ . Peak inward current density (pA/pF) decreased after bath application of 100  $\mu\text{M}$  MB ( $F_{1,6} = 7.8$ ,  $p = 0.031$ ). Post-hoc tests showed that this difference was significant from  $-10$  mV to 60 mV (Figure 3(a)). Peak outward current density (pA/pF) also significantly decreased following exposure to MB ( $F_{1,6} = 13.3$ ,  $p = 0.011$ ). Significant differences occurred for all step levels (Figure 3(b)). Representative traces of current responses before and after MB application are shown in Figure 3(c) and (d). Whereas outward current density decreased after MB, mean resting membrane potential was not altered ( $-53.9 \pm 1.9$  mV to  $-52.5 \pm 2.3$  mV;  $t_9 = 0.66$ ,  $p = 0.529$ ). Action potential

**Figure 2.** Concentration response curve for the proportion of DRG cells without neurite processes used to calculate the EC<sub>50</sub> concentration of methylene blue.

characteristics were calculated at rheobase before and after exposure to MB (Table 2).

MB decreased AP amplitude, AP overshoot, and AP afterhyperpolarization (AHP), and increased AP rise time. Current thresholds, AP fall time, AP width at 0 mV, and AP threshold potential were not altered by MB. Representative examples of individual neurons are shown in Figure 4(a) and (b). Both showed a blunted AP amplitude post-drug, and Figure 4(b) also highlights the decrease in AP afterhyperpolarization.

Responses to current stimulation were decreased overall following MB, but the main effect was not significant ( $F_{1,10} = 3.8$ ,  $p = 0.080$ ). However, there was a significant drug  $\times$  stimulus level interaction ( $F_{2,20} = 4.8$ ,  $p = 0.020$ ). Bonferroni tests indicated that responses following MB application were lower at 3X rheobase (Figure 5(a)). Representative traces of a neuron responding to current stimulation before and after application of MB are shown in Figure 5(b) and (c).

## Discussion

Our results show that exposure to 0.3–10 mM MB produced concentration-dependent absence of neurites in cultured

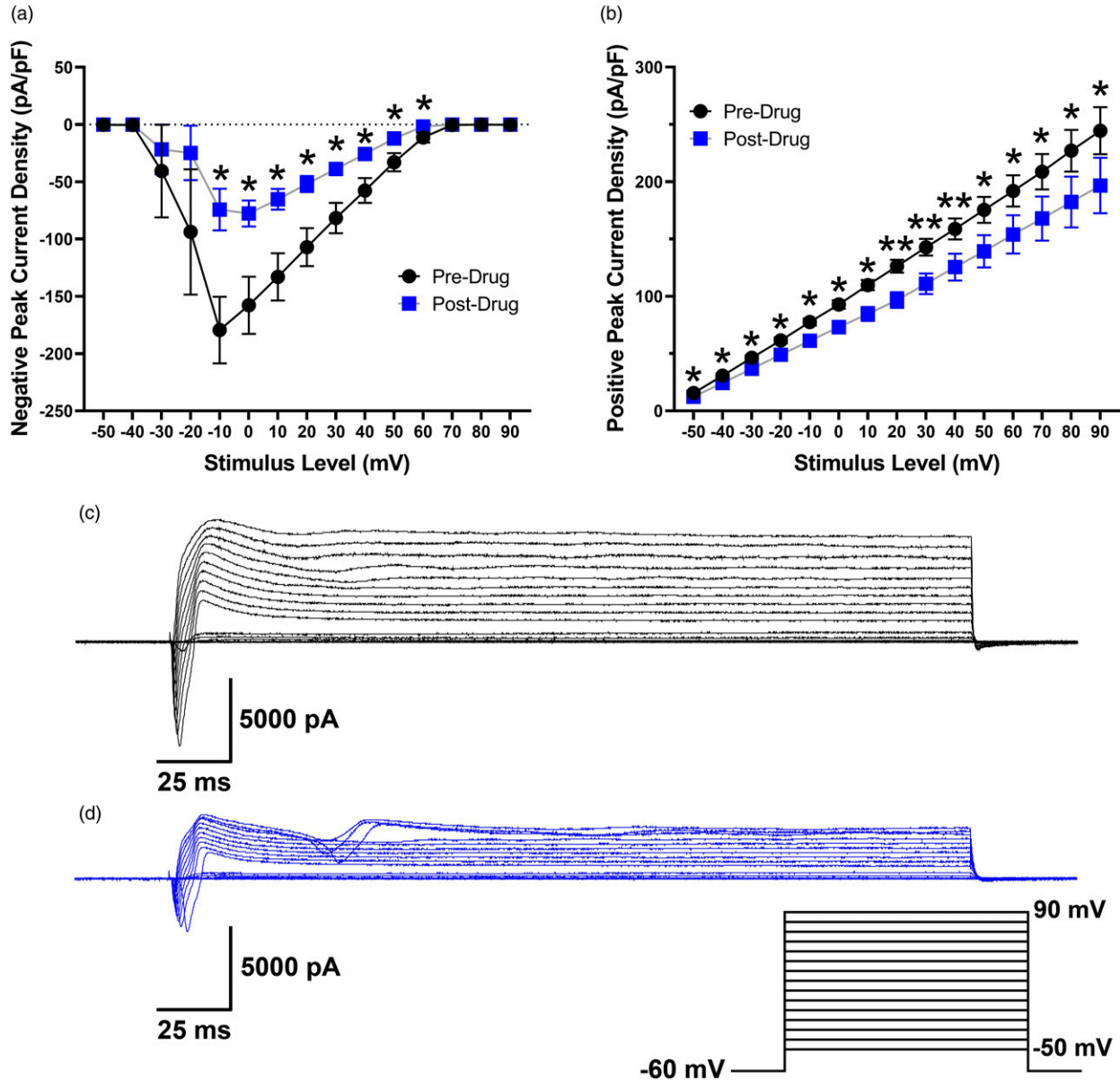


**Figure 3.** Peak negative (A) and positive (B) current density (pA/pF) in rat DRG neurons before and after a 10 min application of MB ( $n = 7$ ). Traces represent current evoked by command voltage step from  $-60$  mV (holding potential) to test potentials between  $-50$  and  $90$  mV in  $10$ -mV increments as shown in the inset for a rat DRG neuron before (C) and after (D) application of MB. \* $p < 0.05$ , \*\* $p < 0.01$ .

mouse DRG neurons. Although the exact etiology is unclear, our results suggest that clinical application of high concentration MB in peripheral nervous tissue is contraindicated. For most clinical applications, a 1% concentration of MB is used for tissue infiltration, which is equivalent to 31.26 mM. Our results are in agreement with previous studies that showed intravenous administration of MB produced neuronal apoptosis in the cerebral cortex of rats,<sup>25</sup> and application of MB *in vitro* led to cell death in rat hippocampal slice preparations and neurite retraction in cultured neurons at concentrations between 1 and 10  $\mu$ M after only a 2-h exposure.<sup>25</sup> Our results are also consistent with clinical studies

showing toxicity following MB administration. For example, MB infusion during parathyroidectomy surgery caused prolonged disorientation in the postoperative period.<sup>37-43</sup> Lumbar intrathecal administration of MB was followed by paraplegia and spinal cord necrosis.<sup>44</sup> Epidural administration of MB also induced paraplegia and inflammation of the spinal cord and nerve roots in cats<sup>28</sup> and quadriplegia associated with spinal inflammation in a patient.<sup>26</sup> The intravenous administration of MB caused toxic encephalopathy-like symptoms, including confusion, aphasia, and disorientation.<sup>37-43,45</sup> The potential neurotoxic side effects of MB are further supported by our observation that acute

**Table 2.** Action potential characteristics of cultured rat DRG neurons before and after a 10 min application of Methylene Blue (100  $\mu$ M).

	Pre-drug	Post-drug	Significance
Dorsal root ganglion neuron action potential characteristics			
Current threshold (pA)	84.5 $\pm$ 26.5 (11)	74.5 $\pm$ 27.9 (11)	n.S. ( $p = 0.38$ )
AP amplitude (mV)	97.4 $\pm$ 2.7 (10)	76.4 $\pm$ 5.4 (10) <sup>***</sup>	$p < 0.005$
AP rise time (ms)	2.8 $\pm$ 0.3 (10)	4.7 $\pm$ 0.4 (10) <sup>***</sup>	$p < 0.005$
AP fall time (ms)	14.7 $\pm$ 2.3 (10)	20.9 $\pm$ 4.7 (10)	n.S. ( $p = 0.08$ )
Width at 0 mV (ms)	6.2 $\pm$ 0.8 (10)	7.2 $\pm$ 1.4 (10)	n.S. ( $p = 0.22$ )
AP overshoot (mV)	52.4 $\pm$ 2.9 (10)	32.4 $\pm$ 6.3 (10) <sup>**</sup>	$p < 0.01$
AP afterhyperpolarization (mV)	11.2 $\pm$ 2.9 (10)	4.5 $\pm$ 1.8 (10) <sup>**</sup>	$p < 0.01$
Threshold potential (mV)	-12.6 $\pm$ 2.1 (10)	-15.0 $\pm$ 4.2 (10)	ns ( $p = 0.44$ )

Data presented as mean  $\pm$  SEM, with the number of neurons in parentheses. AP: action potential. <sup>\*\*</sup> $p < 0.01$ , <sup>\*\*\*</sup> $p < 0.005$ .

treatment with MB impacted membrane electrical properties of cultured rat DRG neurons, with changes in excitability after only 10 min of exposure. MB decreased both positive and negative peak current densities, decreased AP amplitude, AP overshoot, and AP AHP, increased AP rise time, and decreased responses to current stimulation. Notably, while we were able to obtain data 10 min after application of MB, our attempts to assess neuronal activity at 30 min were hindered as the ability to generate an AP was lost or the quality of the patch degraded rapidly, suggesting that acute MB is also neurotoxic at this concentration. We did not assess whether lower concentrations of MB produced a similar effect, and future studies should investigate whether concentrations below the EC<sub>50</sub> of 3.9  $\mu\text{M}$  that we observed in cultured DRGs could minimize its effect on membrane electrical properties in an acute setting. Our results are in line with a previously published report using a lower concentration of

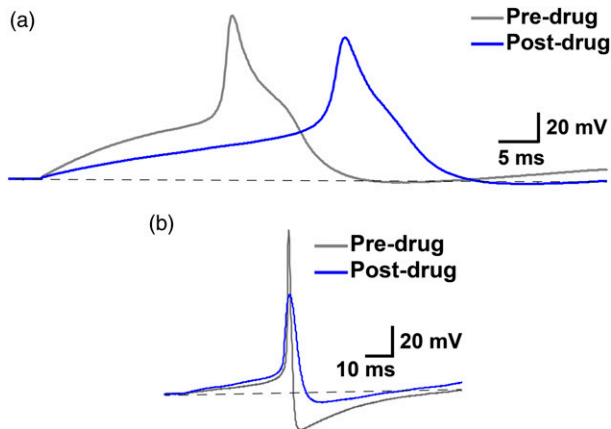


**Figure 4.** Action potential (AP) characteristics in rat DRG neurons ( $n = 10$ ) before and after a 10 min application of methylene blue (100  $\mu\text{M}$ ). Overlapping raw traces from two neurons, one with a shoulder on the falling phase of the action potential (A) and one without (B).

MB (10  $\mu\text{M}$ ), that showed decreased AP amplitude, AP overshoot, and firing frequency in rat hippocampal CA1 pyramidal neurons.<sup>46</sup> In addition, the amplitude of  $I_{\text{Na}}$  following MB was reduced following application of 10 and 100  $\mu\text{M}$ , suggesting that our results could be partially explained by inhibition of voltage-gated sodium channels. We observed decreased peak current density in the current study, but interpretation of these results is limited as we did not test for effects on specific ion channel populations. Changes in neuronal excitability following MB were also found in guinea pig small intestinal myenteric ganglion neurons. In those studies, MB decreased hyperpolarizing after-potentials, depolarized resting membrane potential, and increased input resistance, effects which were partially mediated by the inhibition of inward calcium fluxes.<sup>47</sup> A study in *Xenopus* oocytes expressing the  $\alpha 7$  subunit of the human nicotinic acetylcholine receptor showed that MB inhibited currents induced by acetylcholine with a half-maximal inhibitory concentration (IC<sub>50</sub>) of  $3.4 \pm 0.3 \mu\text{M}$  without affecting endogenous  $\text{Ca}^{2+}$ -dependent  $\text{Cl}^-$  channels.<sup>48</sup> Nicotinic acetylcholine receptor activity in rat CA1 hippocampal pyramidal neurons was also inhibited by 3  $\mu\text{M}$  MB.<sup>48</sup> In the current study, we preferentially studied small-diameter rat DRG neurons, which tend to be nociceptive in nature and exhibit distinct calcium channel function in comparison to medium- and large-diameter neurons in rats, which represent a more heterogeneous population of nociceptive and non-nociceptive cells.<sup>49-52</sup> Future studies should also explore the effect of MB on the membrane electrical properties of these medium- and large-diameter neurons.

In contrast to our results, neuroprotection has been associated with MB.<sup>1,13,53-55</sup> For example, MB was effective as a prophylactic treatment for ifosfamide-induced encephalopathy.<sup>56</sup> In a rat model of traumatic brain injury, 1 mg/kg intravenous MB before or after brain injury attenuated deficits in responses to tactile and proprioceptive stimulation of the contralateral fore and hind paws.<sup>57</sup> In studies *in vitro*, MB

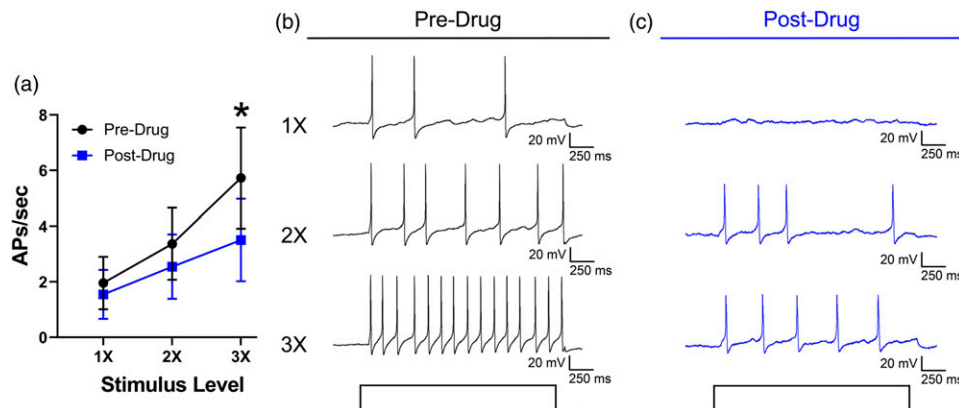


**Figure 5.** (A) Mean responses of rat DRG neurons ( $n = 11$ ) to current stimulation expressed as the number of APs per second at 1X, 2X, and 3X rheobase before and after a 10 min application of methylene blue (100  $\mu\text{M}$ ). Traces represent responses to 1X, 2X, and 3X rheobase current stimulation before (B) and after (C) methylene blue application. \* $p < 0.05$ .

(0.05–1  $\mu\text{M}$ ) increased survival of cerebellar granule neurons in response to mitochondrial toxins.<sup>58</sup> Low concentrations of MB (alone or combined with near-infrared light) protected against neuronal degeneration and improved memory function through effects on mitochondrial electron transport chains.<sup>53,59</sup> Opposing neurological effects of low and high concentrations complicates the clinical picture for the use of MB.<sup>53</sup> As noted above, a generally higher concentration of MB (up to 1%, equivalent to 31.26 mM) is commonly used in most clinical settings.<sup>60,61</sup>

One limitation in the current study is that our experiments were performed using cultured DRG cells. It has been shown that many mRNAs are expressed in the native tissue, but not in cultured cells.<sup>62</sup> We also cannot discount the potential impact of cells that are not present in cultured DRG tissue, such as circulating immune cells that exist in low numbers in naïve tissue that can be activated and infiltrate into DRG and peripheral nerves in response to nerve injury or inflammation, such as macrophages.<sup>63</sup> In this regard, the presence of non-neuronal cells, which could include satellite glial cells, fibroblasts, and a small amount of immune cells (generally representing less than 1% of cells in naïve mouse DRG tissue), helped mitigate the cytotoxic effects of the MB in the present study, and as the native tissues are much more densely packed *in vivo*, this could also impact the effective EC50. An EC50 does not describe an absolute value of toxicity, but instead represents acute toxicity given the exact conditions of the experiment.<sup>36</sup> As such, it is an inherently variable parameter. Given this, accuracy is not able to be quantified and significant importance should be placed on the precision of the measurement.<sup>64</sup> Further studies are needed to determine dose–response relationships for MB in order to mitigate its neurotoxicity in light of its usefulness in clinical settings.

## Significance

An overwhelming number of previous studies emphasized neuroprotective effects of MB in contrast to results presented in this study and others.<sup>25,26,28,37–47</sup> It is likely that MB is neuroprotective at lower dose and toxic at higher doses. Since clinical application generally uses a MB concentration that is much higher than the highest *in vitro* concentration used in the present study (10  $\mu\text{M}$  vs 31.26 mM, or 1%), our results are concerning for the safety profile of MB in clinical applications, particularly those in which MB is administered close to peripheral neurons, such as intradiscal,<sup>65,66</sup> sacroiliac joint and facet joint injections,<sup>67</sup> epidural application after open discectomy,<sup>68</sup> and percutaneous injection close to peripheral nerves.<sup>69</sup> In pharmacokinetic studies using healthy volunteers, an intravenous bolus of MB at 1.4 mg/kg produced a mean plasma concentration of 5  $\mu\text{M}$ <sup>70</sup>, and a bolus of 100 mg MB produced blood concentrations between 1 and 10  $\mu\text{M}$  during the first 30 min after administration.<sup>71</sup> There are two

important limitations in our study, however. First, there may be species differences in MB induced toxicity between rodents and humans. Second, our experiments were done *in vitro*, and whether a similar concentration of MB will produce neurotoxicity *in vivo* is not clear. In conclusion, considering the results presented in this study, use of MB in neuronal structures requires caution and should only be used after a risk-benefit evaluation.

## Acknowledgements

The authors thank Yan Li, PhD (University of Texas MD Anderson Cancer Center, Houston, TX, USA), and Patrick Dougherty, PhD (University of Texas MD Anderson Cancer Center, Houston, TX, USA) for feedback and guidance.

## Author Contributions

Megan L. Uhelski: Conceptualization, Methodology, Formal analysis, Investigation, Writing-Original Draft, Writing-Review & Editing, Review & Editing, Visualization. Malcolm E. Johns: Conceptualization Methodology, Formal analysis, Investigation, Writing- Original Draft, Writing-Review & Editing, Visualization. Alec Horrmann: Investigation, Formal analysis, Sadiq Mohamed: Investigation, Formal analysis, Ayesha Sohail: Investigation, Formal analysis, Iryna A. Khasabova: Formal analysis, Writing-Review & Editing This author helped with interpretation of data and writing the manuscript. Donald A. Simone: Formal analysis, Writing-Review & Editing, Funding acquisition Ratan K. Banik: Conceptualization, Methodology, Formal analysis, Investigation, Writing-Original Draft, Writing-Review & Editing, Visualization, Supervision, Funding acquisition, Project Administration.

## Declaration of conflicting interests

The author(s) declared no potential conflicts of interest with respect to the research, authorship, and/or publication of this article.

## Funding

The author(s) disclosed receipt of the following financial support for the research, authorship, and/or publication of this article: This work was supported by the Department of Anesthesiology, University of Minnesota and Fairview Medical Center, and by NIH grant CA241627 (DAS).

## ORCID iDs

Ayesha Sohail  <https://orcid.org/0000-0001-8597-6122>  
Ratan K Banik  <https://orcid.org/0000-0001-7126-5768>

## References

- Oz M, Lorke DE, Hasan M, Petroianu GA. Cellular and molecular actions of Methylene Blue in the nervous system. *Med Research Reviews* 2011; 31: 93–117.
- Pelgrims J, De Vos F, Van den Brande J, Schrijvers D, Prové A, Vermorken J. Methylene blue in the treatment and prevention of

- ifosfamide-induced encephalopathy: report of 12 cases and a review of the literature. *Br Journal Cancer* 2000; 82: 291–294.
3. Habib AM, Elsherbeny AG, Almehizia RA. Methylene blue for vasoplegic syndrome postcardiac surgery. *Indian J Crit Care Med* 2018; 22: 168–173.
  4. Hanzlik P. Methylene blue as antidote for cyanide poisoning. *JAMA: J Am Med Assoc* 1933; 100: 357–357.
  5. Li J, Chen X, Qi M, Li Y. Sentinel lymph node biopsy mapped with methylene blue dye alone in patients with breast cancer: a systematic review and meta-analysis. *PLoS One* 2018; 13: e0204364.
  6. Dave U, Shousha S, Westaby D. Methylene blue staining: is it really useful in Barrett's esophagus? *Gastrointest Endoscopy* 2001; 53: 333–335.
  7. Mufti G, Shah P, Parkinson M, Riddle P. Diagnosis of clinically occult bladder cancer by in vivo staining with methylene blue. *Br Journal Urology* 1990; 65: 173–175.
  8. Truesdale MD, Elmer-Dewitt M, Sandri M, Schmidt B, Metzler I, Gadzinski A, Stoller ML, Chi T. Methylene blue injection as an alternative to antegrade nephrostography to assess urinary obstruction after percutaneous nephrolithotomy. *J Endourology* 2016; 30: 476–482.
  9. Delport A, Harvey BH, Petzer A, Petzer JP. Methylene blue and its analogues as antidepressant compounds. *Metab Brain Disease* 2017; 32: 1357–1382.
  10. Naylor G, Smith A, Connelly P. A controlled trial of methylene blue in severe depressive illness. *Biol Psychiatry* 1987; 22: 657–659.
  11. Narsapur S, Naylor G. Methylene blue. *J Affective Disorders* 1983; 5: 155–161.
  12. Atamna H, Kumar R. Protective role of methylene blue in Alzheimer's disease via mitochondria and cytochrome c oxidase. *J Alzheimer's Dis* 2010; 20: S439–S452.
  13. Smith ES, Clark ME, Hardy GA, Kraan DJ, Biondo E, Gonzalez-Lima F, Cormack LK, Monfils M, Lee HJ. Daily consumption of methylene blue reduces attentional deficits and dopamine reduction in a 6-OHDA model of Parkinson's disease. *Neuroscience* 2017; 359: 8–16.
  14. Organization WH. *WHO Model List of Essential Medicines, 20th List*, 2017. March 2017, amended August 2017.
  15. Gruetter CA, Kadowitz PJ, Ignarro LJ. Methylene blue inhibits coronary arterial relaxation and guanylate cyclase activation by nitroglycerin, sodium nitrite, and amyl nitrite. *Can Journal Physiology Pharmacology* 1981; 59: 150–156.
  16. Wang Y-X, Cheng X, Pang CCY. Vascular pharmacology of methylene blue in vitro and in vivo: a comparison with NG-nitro-l-arginine and diphenylethylidenehydrazine. *Br J Pharmacol* 1995; 114: 194–202, DOI: [10.1111/j.1476-5381.1995.tb14925.x](https://doi.org/10.1111/j.1476-5381.1995.tb14925.x).
  17. Luo D, Das S, Vincent SR. Effects of methylene blue and LY83583 on neuronal nitric oxide synthase and NADPH-diphosphorase. *Eur J Pharmacol Mol Pharmacol* 1995; 290: 247–251.
  18. Tesfamariam B, Cohen RA. Inhibition of adrenergic vasoconstriction by endothelial cell shear stress. *Circ Research* 1988; 63: 720–725.
  19. Mayer B, Brunner F, Schmidt K. Inhibition of nitric oxide synthesis by methylene blue. *Biochem Pharmacology* 1993; 45: 367–374.
  20. Mayer B, Brunner F, Schmidt K. Novel actions of methylene blue. *Eur Heart Journal* 1993; 14: 22–26.
  21. Pfaffendorf M, Bruning T, Batink H, Van Zwieten P. The interaction between methylene blue and the cholinergic system. *Br J Pharmacol* 1997; 122: 95–98.
  22. Petzer A, Harvey BH, Wegener G, Petzer JP, Azure B. Azure B, a metabolite of methylene blue, is a high-potency, reversible inhibitor of monoamine oxidase. *Toxicol Appl Pharmacol* 2012; 258: 403–409. DOI: [10.1016/j.taap.2011.12.005](https://doi.org/10.1016/j.taap.2011.12.005).
  23. Liao Y-P, Hung D-Z, Yang D-Y. Hemolytic anemia after methylene blue therapy for aniline-induced methemoglobinemia. *Vet Human Toxicology* 2002; 44: 19–21.
  24. Porat R, Gilbert S, Magilner D. Methylene blue-induced phototoxicity: an unrecognized complication. *Pediatrics* 1996; 97: 717–721.
  25. Vutskits L, Briner A, Klauser P, Gascon E, Dayer AG, Kiss JZ, Muller D, Licker MJ, Morel DR. Adverse effects of methylene blue on the central nervous system. *Anesthesiology* 2008; 108: 684–692.
  26. Arieff AJ, Pyzik SW. Quadriplegia after intrathecal injection of methylene blue. *J Am Med Assoc* 1960; 173: 794–796.
  27. Schultz P, Schwarz GA. Radiculomyelopathy Following Intrathecal Instillation of Methylene Blue. *Arch Neurology* 1970; 22: 240–244.
  28. Poppers PJ, Mastri AR, Lebeoux M, Covino BG. The effect of methylene blue on neural tissue. *Anesthesiology* 1970; 33: 335–340.
  29. Ustinova EE, Shurin GV, Gutkin DW, Shurin MR. The role of TLR4 in the paclitaxel effects on neuronal growth in vitro. *PLoS One* 2013; 8: e56886.
  30. Park SH, Eber MR, Fonseca MM, Patel CM, Cunnane KA, Ding H, Hsu F-C, Peters CM, Ko M-C, Strowd RE, Wilson JA, Hsu W, Romero-Sandoval EA, Shiozawa Y. Usefulness of the measurement of neurite outgrowth of primary sensory neurons to study cancer-related painful complications. *Biochem Pharmacol* 2021; 188: 114520.
  31. Lowery LA, Vactor DV. The trip of the tip: understanding the growth cone machinery. *Nat Reviews Mol Cell Biology* 2009; 10: 332–343.
  32. Dickson BJ, Senti K-A. Axon guidance: growth cones make an unexpected turn. *Curr Biol* 2002; 12: R218–R220.
  33. Scott BS. Adult mouse dorsal root ganglia neurons in cell culture. *J Neurobiology* 1977; 8: 417–427.
  34. Li Y, North RY, Rhines LD, Tatsui CE, Rao G, Edwards DD, Cassidy RM, Harrison DS, Johansson CA, Zhang H, Dougherty PM. DRG voltage-gated sodium channel 1.7 is upregulated in paclitaxel-induced neuropathy in rats and in humans with neuropathic pain. *J Neurosci* 2018; 38: 1124–1136.
  35. Akçay A. *The Calculation of LD50 Using Probit Analysis*. Wiley Online Library, 2013.
  36. Krug AK, Balmer NV, Matt F, Schönerberger F, Merhof D, Leist M. Evaluation of a human neurite growth assay as specific

- screen for developmental neurotoxicants. *Arch Toxicol* 2013; 87: 2215–2231. DOI: [10.1007/s00204-013-1072-y](https://doi.org/10.1007/s00204-013-1072-y).
37. Bach KK, Lindsay FW, Berg LS, Howard RS. Prolonged postoperative disorientation after methylene blue infusion during parathyroidectomy. *Anesth Analgesia* 2004; 99: 1573–1574.
  38. Khan M, North A, Chadwick D. Prolonged postoperative altered mental status after methylene blue infusion during parathyroidectomy: a case report and review of the literature. *Ann R Coll Surgeons Engl* 2007; 89: W9–W11.
  39. Kartha SS, Chris CE, Bumpous JM, Fleming M, Lentsch EJ, Flynn MB. Toxic metabolic encephalopathy after parathyroidectomy with methylene blue localization. *Otolaryngology-Head Neck Surg* 2006; 135: 765–768.
  40. Majithia A, Stearns M. Methylene blue toxicity following infusion to localize parathyroid adenoma. *The J Laryngol Otolaryngol* 2006; 120: 138–140.
  41. Martindale S, Stedeford J. Neurological sequelae following methylene blue injection for parathyroidectomy. *Anaesthesia* 2003; 58: 1041–1042.
  42. Sweet G, Standiford SB. Methylene-Blue-Associated Encephalopathy. *J American College Surgeons* 2007; 204: 454–458.
  43. Mihai R, Mitchell EW, Warwick J. Dose-response and post-operative confusion following methylene blue infusion during parathyroidectomy. *Can J Anesthesia/Journal Canadien D'anesthésie* 2007; 54: 79–81.
  44. Sharr MM, Weller RO, Brice JG. Spinal cord necrosis after intrathecal injection of methylene blue. *J Of Neurol Neurosurg Psychiatry* 1978; 41: 384–386. DOI: [10.1136/jnnp.41.4.384](https://doi.org/10.1136/jnnp.41.4.384).
  45. Nadler JE, Green H, Rosenbaum A. Intravenous injection of methylene blue in man with reference to its toxic symptoms and effect on the electrocardiogram. *Am J Med Sci* 1934; 188: 15–21
  46. Zhang Y, Zhao J, Zhang T, Yang Z. In vitro assessment of the effect of methylene blue on voltage-gated sodium channels and action potentials in rat hippocampal CA1 pyramidal neurons. *Neurotoxicology* 2010; 31: 724–729.
  47. Nemeth P, Daly K, Erde S, Wood JD. Effects of methylene blue on electrical behavior of myenteric neurons. *Experientia* 1985; 41: 259–261.
  48. Al Mansouri AS, Lorke DE, Nurulain SM, Ashoor A, Yang Keun-Hang S, Petroianu G, Isaev D, Oz M. Methylene Blue Inhibits the Function of  $\alpha_7$ -Nicotinic Acetylcholine Receptors. *CNS Neurol Disord - Drug Targets* 2012; 11: 791–800. DOI: [10.2174/187152712803581010](https://doi.org/10.2174/187152712803581010).
  49. Julius D, Basbaum AI. Molecular mechanisms of nociception. *Nature* 2001; 413: 203–210. DOI: [10.1038/35093019](https://doi.org/10.1038/35093019).
  50. Scroggs RS, Fox AP. Calcium current variation between acutely isolated adult rat dorsal root ganglion neurons of different size. *J Physiol* 1992; 445: 639–658. DOI: [10.1113/jphysiol.1992.sp018944](https://doi.org/10.1113/jphysiol.1992.sp018944).
  51. Lawson SN, Waddell PJ. Soma neurofilament immunoreactivity is related to cell size and fibre conduction velocity in rat primary sensory neurons. *J Physiol* 1991; 435: 41–63. DOI: [10.1113/jphysiol.1991.sp018497](https://doi.org/10.1113/jphysiol.1991.sp018497).
  52. Lee KH, Chung K, Chung JM, Coggeshall RE. Correlation of cell body size, axon size, and signal conduction velocity for individually labelled dorsal root ganglion cells in the cat. *J Comp Neurol* 1986; 243: 335–346. DOI: [10.1002/cne.902430305](https://doi.org/10.1002/cne.902430305).
  53. Rojas JC, Bruchey AK, Gonzalez-Lima F. Neurometabolic mechanisms for memory enhancement and neuroprotection of methylene blue. *Prog Neurobiol* 2012; 96: 32–45. DOI: [10.1016/j.pneurobio.2011.10.007](https://doi.org/10.1016/j.pneurobio.2011.10.007).
  54. Rojas JC, Simola N, Kermath BA, Kane JR, Schallert T, Gonzalez-Lima F. Striatal neuroprotection with methylene blue. *Neuroscience* 2009; 163: 877–889.
  55. Rojas JC, John JM, Lee J, Gonzalez-Lima F. Methylene blue provides behavioral and metabolic neuroprotection against optic neuropathy. *Neurotoxicity Research* 2009; 15: 260–273.
  56. Turner AR, Duong CD, Good DJ. Methylene Blue for the Treatment and Prophylaxis of Ifosfamide-induced Encephalopathy. *Clin Oncol* 2003; 15: 435–439. DOI: [10.1016/S0936-6555\(03\)00114-6](https://doi.org/10.1016/S0936-6555(03)00114-6).
  57. Stelmashook EV, Genrikhs EE, Mukhaleva EV, Kapkaeva MR, Kondratenko RV, Skrebitsky VG, Isaev NK. Neuroprotective Effects of Methylene Blue In Vivo and In Vitro. *Bull Exp Biol Med* 2019; 167: 455–459. DOI: [10.1007/s10517-019-04548-3](https://doi.org/10.1007/s10517-019-04548-3).
  58. Abe M, Endoh T, Suzuki T. Angiotensin II-induced ionic currents and signalling pathways in submandibular ganglion neurons. *Arch Oral Biol* 2003; 48: 401–413. DOI: [10.1016/S0003-9969\(03\)00041-4](https://doi.org/10.1016/S0003-9969(03)00041-4).
  59. Gonzalez-Lima F, Aucter A. Protection against neurodegeneration with low-dose methylene blue and near-infrared light. *Front Cell Neurosci* 2015; 9: 179. DOI: [10.3389/fncel.2015.00179](https://doi.org/10.3389/fncel.2015.00179).
  60. Özdemir A, Mayir B, Demirbakan K, Oygür N. Efficacy of methylene blue in sentinel lymph node biopsy for early breast cancer. *Journal Breast Health* 2014; 10: 88.
  61. Dumbarton TC, Gorman SK, Minor S, Loubani O, White F, Green R. Local cutaneous necrosis secondary to a prolonged peripheral infusion of methylene blue in vasodilatory shock. *Ann Pharmacotherapy* 2012; 46: e6.
  62. Wangzhou A, McIlvried LA, Paige C, Barragan-Iglesias P, Guzman CA, Dussor G, Ray PR, Gereau RW, Price TJ. Transcriptomic analysis of native versus cultured human and mouse dorsal root ganglia focused on pharmacological targets. *BioRxiv* 2019; 2019: 766865.
  63. Scholz J, Woolf CJ. The neuropathic pain triad: neurons, immune cells and glia. *Nat Neurosci* 2007; 10: 1361–1368. DOI: [10.1038/nn1992](https://doi.org/10.1038/nn1992).
  64. Walum E. Acute oral toxicity. *Environ Health Perspect* 1998; 106: 497–503. DOI: [doi:10.1289/ehp.98106497](https://doi.org/10.1289/ehp.98106497).
  65. Guo X, Ding W, Liu L, Yang S. Intradiscal Methylene Blue Injection for Discogenic Low Back Pain: A Meta-Analysis. *Pain Pract* 2019; 19: 118–129. DOI: [10.1111/papr.12725](https://doi.org/10.1111/papr.12725).
  66. Kim SH, Ahn SH, Cho YW, Lee DG. Effect of Intradiscal Methylene Blue Injection for the Chronic Discogenic Low Back Pain: One Year Prospective Follow-up Study. *Ann Rehabil Med* 2012; 36: 657–664. DOI: [10.5535/arm.2012.36.5.657](https://doi.org/10.5535/arm.2012.36.5.657).

67. Parekh J, Eckmann M, Ramamurthy S. Case Series of Methylene Blue Injections for the Treatment of Zygapophysial and Sacroiliac Joint Pain: Results of 5 Cases. *Open J Anesthesiology* 2013; 03: 301–303.
68. Farrokhi MR, Lotfi M, Masoudi MS, Gholami M. Effects of methylene blue on postoperative low-back pain and functional outcomes after lumbar open discectomy: a triple-blind, randomized placebo-controlled trial. *J Neurosurg Spine* 2016; 24: 7–15. DOI: [10.3171/2015.3.Spine141172](https://doi.org/10.3171/2015.3.Spine141172).
69. Osorio JA, Breshears JD, Arnaout O, Simon NG, Hastings-Robinson AM, Aleshi P, Kliot M. Ultrasound-guided percutaneous injection of methylene blue to identify nerve pathology and guide surgery. *Neurosurg Focus* 2015; 39: E2. DOI: [10.3171/2015.6.Focus15220](https://doi.org/10.3171/2015.6.Focus15220).
70. Aeschlimann C, Cerny T, Küpfer A. Inhibition of (mono) amine oxidase activity and prevention of ifosfamide encephalopathy by methylene blue. *Drug Metabolism Disposition: The Biological Fate Chemicals* 1996; 24: 1336–1339.
71. Peter C, Hongwan D, Küpfer A, Lauterburg B. Pharmacokinetics and organ distribution of intravenous and oral methylene blue. *Eur Journal Clinical Pharmacology* 2000; 56: 247–250.